

[Fe IV] Emission in Ionized Nebulae

Mónica Rodríguez

*Instituto Nacional de Astrofísica, Óptica y Electrónica INAOE, Apdo Postal 51 y 216,
72000 Puebla, Pue., Mexico*

mrodri@inaoep.mx

ABSTRACT

This paper presents an analysis of [Fe IV] emission based on new identifications and previous measurements of [Fe IV] lines in 30 Doradus, IC 4846, M42, SMC N88A, and SBS 0335–052. The Fe abundances obtained by adding the abundances of the relevant Fe ions (mainly Fe^{++} and Fe^{3+}) are found to be lower, by factors in the range 2.6–5.9, than the Fe abundances implied by [Fe III] emission and an ionization correction factor derived from ionization models. The most likely explanation of this discrepancy is that either the collision strengths for [Fe IV] or the Fe ionization fractions predicted by models are unreliable. The available data neither allow one to distinguish between these two possibilities nor to exclude another possible explanation: that the discrepancy implies the presence of a gradient in the Fe abundance within the ionized gas. Further measurements of [Fe IV] lines and checks on the Fe^{3+} atomic data and ionization models are needed to reach a definitive conclusion. The discrepancy introduces an uncertainty in the determination of Fe abundances in ionized nebulae. This uncertainty has implications for our understanding of both the evolution of dust in ionized nebulae and the chemical history of low metallicity galaxies.

Subject headings: H II regions — line: identification — ISM: abundances

1. INTRODUCTION

The first detection of an [Fe IV] line in an H II region is due to Rubin et al. (1997), who measure [Fe IV] $\lambda 2836.56$ in the UV spectrum of the Orion nebula (M42). From this line and two previous ionization models for Orion, Rubin et al. find Fe/H lower, by factors of 6.5 and 19, than the value the models need to reproduce [Fe II] and [Fe III] emission in M42, $\text{Fe}/\text{H} = 3 \times 10^{-6}$. According to Rubin et al., the difference between the results obtained from the two models is due mostly to the different average electron temperatures (T_e) predicted by

each model. Since the two Orion models and the measurement of the [Fe IV] line correspond to different regions in the nebula, an underlying assumption in the above comparison is that the gaseous Fe abundance remains roughly constant within the ionized gas.

On the other hand, Rodríguez (2002) calculates the Fe abundances for 12 regions in M42 from the Fe^+ and Fe^{++} abundances and ionization correction factors (ICFs) for the contribution of Fe^{3+} , obtained from grids of photoionization models. Since the Fe^+ abundance is very low for all positions ($\text{Fe}^+/\text{Fe}^{++} < 0.3$), the results depend mostly on the derived Fe^{++} abundances, and these are based on the atomic data leading to the best fit between the observed and predicted relative intensities of the [Fe III] lines. The final Fe abundances are lower than those derived in previous studies based on older atomic data, and show variations of more than a factor of 2: $\text{Fe}/\text{H} = 0.8\text{--}1.8 \times 10^{-6}$. Taking this into account, the discrepancy found by Rubin et al. (1997) could be reduced and now gets as close as a factor of ~ 2 , and Rodríguez (2002) argues that given all the uncertainties involved in the calculations, this discrepancy might not be significant. The main uncertainties arise from the calculation of the Fe^{3+} abundance from one weak UV line, which is very sensitive to T_e and the extinction correction, and from the lack of measurements of [Fe II], [Fe III], and diagnostic lines at exactly the same position in the nebula. The measurement of optical [Fe IV] lines would solve this difficulty, but these lines are weak and difficult to observe. Since Fe^{3+} is an important or dominant ionization state in most H II regions, the reality of this underabundance implied by [Fe IV] emission, and the reasons behind it, are critical issues in our understanding of both the evolution of dust in H II regions (see Rodríguez 2002) and the chemical evolution at low metallicities (see Izotov & Thuan 1999).

This paper presents the identification and analysis of one [Fe IV] line at $\lambda 6739.8$ in the optical spectra of M42 observed by Baldwin et al. (2000). The same line is identified in the spectra of the planetary nebula IC 4846 (Hyung et al. 2001). Upper limits to the intensities of [Fe IV] $\lambda\lambda 6734.4, 6739.8$ are obtained from the spectra of 30 Doradus in the LMC observed by Peimbert (2003). Another optical [Fe IV] line at $\lambda \sim 4904$, tentatively identified by Izotov, Chaffee & Schaerer (2001) in the spectra of the blue compact dwarf galaxy SBS 0335–052, and the measurement of [Fe IV] $\lambda 2836.56$ in SMC N88A by Kurt et al. (1999) are used to complete a set of data in which to perform an analysis of [Fe IV] emission and the Fe abundance in different ionized nebulae.

2. [Fe IV] LINES IN SEVERAL OBJECTS

Throughout this paper air wavelengths are used for the optical lines and vacuum wavelengths for the UV ones. The transitions giving rise to the [Fe IV] lines discussed here are

identified in Figure 1 (see also Table 1).

The deepest optical spectrum of M42 has been published by Baldwin et al. (2000). They find a weak feature at $\lambda 6739.86$ which they consider as clearly detected but unidentified. The line has an extinction-corrected relative intensity of $I(\lambda 6739.86)/I(\text{H}\beta) = 3.7 \times 10^{-5}$. The wavelength is very close to [Fe IV] $\lambda 6739.8$ (${}^2I_{11/2} \rightarrow {}^4G_{11/2}$), the brightest optical [Fe IV] line that can be expected to form at the physical conditions prevailing in M42. This line was previously identified in the spectrum of NGC 7027 (Baluteau et al. 1995), one of the most dense and luminous planetary nebulae, which has an extremely rich spectrum. For the Orion observations the agreement in wavelength is very good, especially when accounting for the difference of $\sim 2 \text{ km s}^{-1}$ due to the trend of velocity vs. ionization potential found by Baldwin et al. (2000). The measurements of [Fe IV] $\lambda 2836.56$ by Rubin et al. (1997) and [Fe IV] $\lambda 6739.8$ by Baldwin et al. (2000) were performed at different positions in Orion, but both positions are at similar distances from the ionizing star θ^1 Ori C ($32''$ and $37''$, respectively), so that it might be instructive to compare their intensities. The reddening-corrected intensities relative to H β of both lines imply $I(\lambda 6739.8)/I(\lambda 2836.56) = 0.039$, whereas for typical Orion physical conditions (see Table 2 and §3 below) the expected value of this ratio is $\simeq 0.022$. Other optical [Fe IV] lines following $\lambda 6739.8$ in intensity would be $\lambda 4906.56$ (${}^4F_{9/2} \rightarrow {}^4G_{11/2}$), $\lambda 6734.4$ (${}^2I_{13/2} \rightarrow {}^4G_{11/2}$), and $\lambda 6761.3$ (${}^2I_{11/2} \rightarrow {}^4G_{9/2}$), but these lines have expected intensities of about half the $\lambda 6739.8$ intensity and they are at the limit of line detection of Baldwin et al. (2000). We have then a good case for the detection of the first optical [Fe IV] line in M42.

A literature search for other nebulae in which to perform an analysis of [Fe IV] emission and the Fe abundance yielded four suitable objects: IC 4846, 30 Doradus, SBS 0335–052, and SMC N88A. Available spectra of these objects include one [Fe IV] line, one or more [Fe III] lines, and the [O II], [O III], and [S II] lines needed to derive T_e values and electron density (N_e) values, the O abundance, and the degree of ionization O^+/O . The optical [Fe IV] lines measured by Esteban et al. (2002) in NGC 2363 and NGC 5471 could not be used because the [O II] $\lambda 3727$ lines were outside their observed wavelength range. Other objects, like the symbiotic nova RR Telescopii, where several [Fe IV] lines have been detected (see, for example, McKenna et al. 1997), were excluded because the high densities responsible for their rich spectra ($N_e \sim 10^6 \text{ cm}^{-3}$) prevent the application of the usual diagnostics.

IC 4846 is a compact planetary nebula, where Hyung, Aller & Lee (2001) measure an unidentified feature at $\lambda 6739.14$. The difference in wavelength with [Fe IV] $\lambda 6739.8$ is compatible with the differences that Hyung et al. find for other well identified lines. Since [Fe IV] $\lambda 6739.8$ is the brightest optical [Fe IV] line for the physical conditions in IC 4846 (see Table 2), this is a likely identification for the measured line. The relative intensity of

the line after the correction for extinction is $I(\lambda 6739.14)/I(\text{H}\beta) = 3.1 \times 10^{-4}$.

The spectra of 30 Doradus observed by Peimbert (2003) shows a line at $\lambda \sim 6734$ that he identifies as [Cr IV] $\lambda 6733.9$ with a possible contribution of C II] $\lambda 6734$. Since for the physical conditions of this object (see Table 2) [Fe IV] $\lambda 6734.4$ (${}^2I_{13/2} \rightarrow {}^4G_{11/2}$) would be the brightest optical [Fe IV] line, the measured feature could have a contribution from this line and the intensity of the feature can be used to obtain an upper limit to the Fe^{3+} abundance. However, a lower upper limit can be obtained by noting the absence of [Fe IV] $\lambda 6739.8$, the optical line that should follow [Fe IV] $\lambda 6734.4$ in intensity, and taking as an upper limit to its intensity the intensity measured for a nearby weak line, [Cr IV] $\lambda 6747.5$: $I(\lambda 6739.8)/I(\text{H}\beta) \leq 1.05 \times 10^{-4}$. There is a feature at $\lambda 5032.4$ identified by Peimbert (2003) as partly due to [Fe IV] $\lambda 5032.4$ (${}^2F_{5/2} \rightarrow {}^4G_{7/2}$), but this line should have a negligible intensity at low densities according to the current atomic data and, therefore, the identification seems unlikely.

The blue compact dwarf galaxy SBS 0335–052 has been observed by Izotov et al. (2001), who tentatively identify a line measured at $\lambda 4904$ as [Fe IV] $\lambda 4906.56$. Given the low spectral resolution, 8 \AA , and considering the physical conditions in SBS 0335–052 (see Table 2), the line is most likely a blend of three [Fe IV] lines in the multiplet: $\lambda 4899.97$ (${}^4F_{7/2} \rightarrow {}^4G_{9/2}$), $\lambda 4903.07$ (${}^4F_{7/2} \rightarrow {}^4G_{7/2}$), and $\lambda 4906.56$ (${}^4F_{9/2} \rightarrow {}^4G_{11/2}$). Two of the unidentified features measured by Izotov et al. (2001), at $\lambda 5235$ and $\lambda 7224$, could also be [Fe IV] lines: $\lambda 5233.76$ (${}^2F_{7/2} \rightarrow {}^4G_{9/2}$), and $\lambda 7222.8$ (${}^4F_{9/2} \rightarrow {}^4D_{7/2}$). The intensities of these two lines relative to the blend at $\lambda 4904$ are consistent with the expected values within a factor of 2 (see Table 1). Other [Fe IV] lines that could be present in the spectrum of SBS 0335–052 are likely to be blended with stronger lines. Since the uncertainties assigned by Izotov et al. (2001) to the intensities of the weak lines are $\sim 100\%$, no further assessment can be made on the reliability of the relative line intensities predicted by the atomic data for [Fe IV]. The Fe^{3+} abundance in this object will be derived from the strongest feature, the [Fe IV] blend at $\lambda 4904$, which Izotov et al. (2001) consider as clearly detected. The extinction-corrected intensity of this feature relative to $\text{H}\beta$ is $I(\lambda 4904)/I(\text{H}\beta) = 2.2 \times 10^{-3}$.

The UV and optical spectra of the Small Magellanic Cloud H II region SMC N88A have been obtained by Kurt et al. (1999), who measure [Fe IV] $\lambda 2836.56$ at two positions in the nebula. The values for the extinction-corrected line ratios are $I(\lambda 2837)/I(\text{H}\beta) = 2.5 \times 10^{-2}$ and 2.4×10^{-2} for the positions identified as bar and square A both in their paper and here.

3. RESULTS

3.1. Atomic Data

The calculations for [Fe IV] used throughout this paper are based on a 33-level model-atom where all collisional and downward radiative transitions are considered. The collision strengths are those calculated by Zhang & Pradhan (1997), the transition probabilities those recommended by Froese Fischer & Rubin (1998) (and those from Garstang 1958 for those transitions not considered by Froese Fischer & Rubin), and the level energies have been taken from the NIST database¹. The calculations for [Fe III] are based on a 34-level model-atom that uses the collision strengths of Zhang (1996) and the transition probabilities of Quinet (1996). The physical conditions and the abundances of the O ions have been derived with the *nebular* package in IRAF.

3.2. Errors and Uncertainties

The abundances presented here are affected by the usual uncertainties related to the method of calculation: (i) the assumption that the observed lines originate in one or two emitting layers of constant N_e and T_e , (ii) the uncertainties in the atomic data used to derive physical conditions and ionic abundances, (iii) errors in the line intensities, and (iv) the uncertainties arising from the use of ICFs to account for unseen stages of ionization.

The systematic uncertainties arising from any of these causes are very difficult to estimate. The errors presented here have been calculated by considering only the errors in the line intensities, following the guidelines given by the different authors for each object, but taking 5% as the minimum error for any line intensity relative to $H\beta$. It should be kept in mind that the errors in the line intensity ratios are just estimates, and that the criteria followed by the different authors may vary. The errors for each calculated quantity have been derived by adding quadratically the errors in the line intensity ratio used to derive the ionic abundance and the errors arising from the uncertainties in both T_e and N_e . The last ones are especially important for the O^+ abundance and all ratios involving this ion (e.g. O^+/O^{++} , Fe^{++}/O^+). Thus, the calculated errors can be used to assess the sensitivity of each quantity to the adopted uncertainties.

¹Available at http://Physics.nist.gov/cgi-bin/AtData/main_asd.

3.3. Physical Conditions and Ionic Abundances

Several diagnostic lines were available for 30 Doradus, IC 4846 and M42. For these objects the T_e obtained from the diagnostic [N II] and [O III] lines have been used to derive the ionic abundances of the low and high ionization species, respectively. The values of the [N II] and [O III] T_e are listed in Table 2. The N_e values listed for these three objects have been derived from the [S II], [O II], [Cl III], and [Ar IV] diagnostic lines. Table 2 shows the mean and standard deviation of the N_e values obtained from the different line ratios. For SMC N88A and SBS 0335–052 the values used for T_e and N_e were those derived from the [O III] and [S II] diagnostic lines. The upper limit of N_e [S II] in SMC-N88A bar was unconstrained with the errors found for the ratio of [S II] lines $I(\lambda 6716)/I(\lambda 6731)$. The upper limit of N_e provided in Table 2 for this object was obtained from the constraints imposed on N_e by other line ratios.

Table 1 shows the [Fe III] and [Fe IV] lines used for the determination of the Fe^{++} and Fe^{3+} abundances in the different objects. In 30 Doradus and M42, 13 to 14 [Fe III] lines were considered to be unblended and available for the abundance determination. The mean values and standard deviations of the calculated Fe^{++} abundances are $\text{Fe}^{++}/\text{H}^+ = 1.67 \pm 0.21 \times 10^{-7}$ for 30 Doradus and $\text{Fe}^{++}/\text{H}^+ = 3.29 \pm 0.21 \times 10^{-7}$ for M42. The agreement between the lines is extremely good, suggesting that the atomic data used for Fe^{++} are quite reliable (see also Rodríguez 2002). As for the other objects, three [Fe III] lines could be used for IC 4846 and just one, [Fe III] $\lambda 4658.1$, for SMC N88A and SBS 0335–052. [The intensity given by Izotov et al. 2001 for [Fe III] $\lambda 5270.4$ in SBS 0335–052 is clearly wrong, as can be seen by inspecting their Fig. 1, but the weaker [Fe III] $\lambda 4754.7$ line agrees to within 10% with the Fe^{++} abundance implied by [Fe III] $\lambda 4658.1$ (see Table 1).]

The intensities measured by Kurt et al. (1999) for [Fe IV] $\lambda 2836.56$ in SMC N88A could have a contribution from C II $\lambda\lambda 2837.5, 2838.4$. In M42, these recombination lines account for nearly 90% of the blend intensity (Rubin et al. 1997). The contribution of the C II lines to the $\lambda 2837$ feature in SMC N88A can be estimated using the recombination coefficients of Davey et al. (2000) and the C^{++} abundances derived by Kurt et al. from C III] $\lambda 1909$. Taking into account that in H II regions the C^{++} abundances implied by recombination lines are usually a factor ~ 2 higher than those derived from collisionally excited lines (see, for example, Table 6 in Esteban et al. 2002), I estimate that the contribution of the C II lines to the intensity measured for [Fe IV] $\lambda 2836.56$ in SMC N88A is below 10%. This contribution will be neglected in what follows.

The large difference between the relative intensities of the [Fe IV] and C II lines in M42 and SMC N88A arises from the lower metallicity of the latter (by a factor ~ 3.5 in the O abundance, see Table 3) and its associated higher T_e . The intensity of the C recombination

lines decreases because of the lower metallicity and higher T_e , whereas the intensity of the forbidden line increases because its emissivity shows an exponential dependence on T_e . The same argument can be used to rule out any significant contamination of either [Fe III] $\lambda 4658.1$ or [Fe IV] $\lambda 4904$ by O II $\lambda 4661.63$ and O II $\lambda 4906.83$ in SMC N88A and SBS 0335–052. In SBS 0335–052, this conclusion is further confirmed by the overall agreement shown by the other [Fe III] and [Fe IV] lines (see Table 1).

The final adopted values for the ionic abundances of O^+ , O^{++} , Fe^{++} , and Fe^{3+} are listed in Table 2.

3.4. Total Abundances

The ion Fe^+ , whose ionization potential is 16.2 eV, can make some contribution to the Fe abundance. Although most of the [Fe II] lines in H II regions are affected by fluorescence effects (Rodríguez 1999a, and references therein), an estimate of the Fe^+ contribution to the total Fe abundance can be obtained from the intensity of [Fe II] $\lambda 8617$, a line almost insensitive to the effects of UV pumping. This line is either undetected or out of the wavelength range measured for the objects considered here. An estimate of the Fe^+ abundance in M42 was obtained by averaging the values of Fe^+/H^+ found in Rodríguez (2002) for three regions in M42 that are $27''$ south of the position observed by Baldwin et al. (2000), but at a similar distance from θ^1 Ori C. The resulting value, $Fe^+/H^+ = 5.4 \pm 2.7 \times 10^{-8}$, is just $\sim 15\%$ of the abundance derived for Fe^{++} . This estimate of the Fe^+ abundance in M42 has been used in the analysis described below, which leads to a discrepancy between the expected and measured values of the Fe^{3+} abundance of a factor 4.4. If Fe^+ had been neglected in this analysis, the discrepancy would be lower, a factor 3.8. Since the other objects have a higher degree of ionization than M42, the contribution of Fe^+ to their Fe abundance will be neglected. The effect of neglecting the Fe^+ abundance in the results for these higher ionization objects is likely to be even lower than for M42, especially for IC 4846 and SMC N88A, where no [Fe II] lines are detected. In any case, if the concentration of Fe^+ in any of these objects were not negligible, the discrepancy between the expected and calculated values of Fe^{3+} would be higher than the values given below.

On the other hand, IC 4846 and SBS 0335–052 show He II emission in their spectra. Since He^+ , O^{++} and Fe^{3+} have similar ionization potentials (54.4, 54.9, and 54.8 eV, respectively), the presence of He^{++} suggests that O^{3+} and Fe^{4+} might also be present. In fact, SBS 0335–052 shows emission in [Fe V] $\lambda 4227$ and, possibly, in some [Fe VI] and [Fe VII] lines whose origin is not clear (Izotov et al. 2001). The [Fe V] $\lambda 4227$ line cannot be used at the moment to derive the Fe^{4+} abundance, since the required atomic data are

not available. However, the amount of He^{++} is low in SBS 0335–052 ($\text{He}^{++}/\text{He}^+ \simeq 0.025$) and lower in IC 4846 ($\text{He}^{++}/\text{He}^+ \simeq 0.0053$), suggesting that the concentrations of O^{3+} and Fe^{4+} are negligible. Therefore, it will be assumed that $\text{O}/\text{H} = \text{O}^+/\text{H}^+ + \text{O}^{++}/\text{H}^+$ and $\text{Fe}/\text{H} = \text{Fe}^{++}/\text{H}^+ + \text{Fe}^{3+}/\text{H}^+$ (except for M42 where $\text{Fe}/\text{H} = \text{Fe}^+/\text{H}^+ + \text{Fe}^{++}/\text{H}^+ + \text{Fe}^{3+}/\text{H}^+$, with $\text{Fe}^+/\text{H}^+ = 5.4 \pm 2.7 \times 10^{-8}$).

Table 3 shows the values of the total abundances for all the objects. Two values are given for the Fe abundance. The first one has been derived from [Fe III] and an ICF, $\text{Fe}/\text{H} = 1.1 [(\text{Fe}^+ + \text{Fe}^{++})/\text{O}^+] \text{O}/\text{H}$. The ICF is based on the grids of ionization models of Stasińska (1990) and Gruenwald & Viegas (1992), and is further discussed in §4 below. The second value for the Fe abundance is just the sum of the derived ionic abundances, $\text{Fe}/\text{H} = \text{Fe}^+/\text{H}^+ + \text{Fe}^{++}/\text{H}^+ + \text{Fe}^{3+}/\text{H}^+$. The Fe abundances based on the sum of the ionic abundances can be seen to be systematically lower, by factors in the range 2.6–5.9, than those implied by the Fe^{++} abundance and an ICF. The expected values of the Fe^{3+} abundance, $\text{Fe}_{\text{exp}}^{3+}$, can be obtained from the relation $\text{Fe}^+/\text{H}^+ + \text{Fe}^{++}/\text{H}^+ + \text{Fe}_{\text{exp}}^{3+}/\text{H}^+ = 1.1 [(\text{Fe}^+ + \text{Fe}^{++})/\text{O}^+] \text{O}/\text{H}$. The values found for $\text{Fe}_{\text{exp}}^{3+}/\text{Fe}^{3+}$ are shown in Table 3: the derived Fe^{3+} abundances are lower than expected by factors ≥ 2.7 (30 Doradus), 3.2 (IC 4846), 4.4 (M42), 5.5 (SMC N88A bar), 7.5 (SMC N88A square A), and 6.1 (SBS 0335–052).

4. IONIZATION CORRECTION FACTORS

The above comparison between the expected and calculated values of $\text{Fe}^{3+}/\text{H}^+$ relies on the ICF applied to the Fe^{++} abundance in order to obtain the total Fe abundance. Since [Fe III] lines are the Fe lines most easily detected in H II regions, this ICF is a key parameter in the determination of the Fe abundance in these nebulae. The O ions are probably the best choice for defining ICFs for the Fe ions. First, because both O^+ and O^{++} can be easily measured from strong optical lines. Second, because the ionization potentials for the Fe and O ions are not too far apart; 16.2, 30.6, and 54.8 eV for Fe^+ , Fe^{++} , and Fe^{3+} ; 13.6, 35.1, and 54.9 eV for O^0 , O^+ and O^{++} . The relations between the Fe and O ions and the Fe/O abundance ratio can be expressed in the following way:

$$\frac{\text{Fe}}{\text{O}} = \left[\frac{x(\text{O}^+)}{x(\text{Fe}^{++})} \right] \frac{\text{Fe}^{++}}{\text{O}^+}, \quad (1)$$

$$\frac{\text{Fe}}{\text{O}} = \left[\frac{x(\text{O}^+)}{x(\text{Fe}^+ + \text{Fe}^{++})} \right] \frac{\text{Fe}^+ + \text{Fe}^{++}}{\text{O}^+}, \quad (2)$$

$$\frac{\text{Fe}}{\text{O}} = \left[\frac{x(\text{O}^{++})}{x(\text{Fe}^{3+})} \right] \frac{\text{Fe}^{3+}}{\text{O}^{++}}, \quad (3)$$

where $x(X)$ is the ionization fraction for the corresponding ion, and the quantities in square brackets are ICFs that will be constant if the ionization fractions of Fe and O vary in similar ways.

The values of the ICFs $[x(\text{O}^+)/x(\text{Fe}^{++})]$, $[x(\text{O}^+)/x(\text{Fe}^+ + \text{Fe}^{++})]$, and $[x(\text{O}^{++})/x(\text{Fe}^{3+})]$ are shown in Figure 2 as a function of O^+/O^{++} for the two series of models calculated by Gruenwald & Viegas (1992) and Stasińska (1990). The ionization models from Gruenwald & Viegas (1992) have metallicities Z_\odot , $Z_\odot/3$, $Z_\odot/10$, and $Z_\odot/100$, electron densities of 10, 100, and 1000 cm^{-3} , and are ionized by a single star with effective temperature $T_{\text{eff}} = 30900$ or 50000 K . The models from Stasińska (1990) considered in Figure 2 are those ionized by one star for Z_\odot and $Z_\odot/2$, and those ionized by 1, 10^2 or 10^4 stars for $Z_\odot/5$, $Z_\odot/10$, and $Z_\odot/50$. These models have N_e of 10 and 1000 cm^{-3} , and $T_{\text{eff}} = 32500\text{--}55000 \text{ K}$. The main difference between the two series is that the results of Gruenwald & Viegas (1992) are presented for several lines of sight across each model.

The results from the two series of models shown in Figure 2 can be compared with those of three individual models for M42: $\log[x(\text{O}^+)/x(\text{Fe}^{++})] = 0.26$ (Baldwin et al. 1991), $\log[x(\text{O}^+)/x(\text{Fe}^{++})] = 0.15$ (Rubin et al. 1991a,b), and $\log[x(\text{O}^+)/x(\text{Fe}^{++})] = 0.04$ (Bautista & Pradhan 1998). The last result has been calculated with the most recent values for the photoionization cross-sections and recombination-rate coefficients for the Fe ions (Nahar 1996a,b), and is similar to the ICF used here.

Figure 2 also shows the results obtained here for the five studied objects (the filled squares for IC 4846, M42, SMC N88A, and SBS 0335–052; the lower and upper limits for 30 Doradus) by assuming that $\text{Fe}/\text{H} = \text{Fe}^+/\text{H}^+ + \text{Fe}^{++}/\text{H}^+ + \text{Fe}^{3+}/\text{H}^+$.

Several comments can be made about Figure 2:

1. The results for those models of Gruenwald & Viegas (1992) with solar metallicity deviate from the relation followed by the models with lower metallicities. This suggests that the ICFs might be dependent on metallicity, but the models of Stasińska (1990) and the results of Gruenwald & Viegas (1992) for subsolar metallicities do not show such dependence.
2. Although the results for each series of models are consistent with roughly constant values for $[x(\text{O}^+)/x(\text{Fe}^{++})]$ and $[x(\text{O}^+)/x(\text{Fe}^+ + \text{Fe}^{++})]$, the values are different for each series.

3. The values of $[x(\text{O}^+)/x(\text{Fe}^{++})]$ are substantially higher than those of $[x(\text{O}^+)/x(\text{Fe}^+ + \text{Fe}^{++})]$. This is due to the fact that the models predict a significant concentration of Fe^+ , although with great scatter: $0.05 < (\text{Fe}^+/\text{Fe}^{++}) < 0.7$. However, the values found in Rodríguez (2002) for Galactic H II regions with $\log(\text{O}^+/\text{O}^{++}) < 0$ for $\text{Fe}^+/\text{Fe}^{++}$ are all lower than 0.3 and mostly around 0.1. The concentrations of ions with low ionization potential like Fe^+ are very model-dependent and, therefore, difficult to estimate with reliability. Furthermore, as suggested by the referee, this difference between the expected and calculated concentrations of Fe^+ can be due to the presence of significant amounts of Fe^+ in neutral zones, where the T_e is too low to produce the optical [Fe II] lines. Therefore, I consider it more reliable to use the ICF implied by $[x(\text{O}^+)/x(\text{Fe}^+ + \text{Fe}^{++})]$, neglecting the contribution of Fe^+ for the high-ionization objects. As discussed above, this should be a good approximation for IC 4846 and SMC N88A, where no [Fe II] lines are detected. If the contribution of Fe^+ were higher than assumed, the discrepancy between the expected and calculated values of Fe^{3+} would be even higher than the values derived here. The calculated results are in any case systematically below the expected ones.
4. According to both series of models, $[x(\text{O}^{++})/x(\text{Fe}^{3+})] \simeq 1$ for $\log(\text{O}^+/\text{O}^{++}) < 0$, and therefore $\text{Fe}^{3+}/\text{O}^{++} \simeq \text{Fe}/\text{O}$ to within 0.1 dex. Since Fe^{3+} and O^{++} are formed at 30.6 and 35.1 eV, and are ionized at 54.8 and 54.9 eV, for those conditions with $x(\text{O}^{++}) \geq 0.9$, most of Fe should be present as Fe^{3+} . Therefore, barring large errors in the atomic data used to derive the Fe ionization balance, $\text{Fe}^{3+}/\text{O}^{++} \simeq \text{Fe}/\text{O}$ should be a very good approximation for high-ionization objects; whereas for any degree of ionization it should hold that $\text{Fe}^{3+}/\text{O}^{++} \geq \text{Fe}/\text{O}$. However, as seen in Figure 2c, all the objects show $\text{Fe}^{3+}/\text{O}^{++} < \text{Fe}/\text{O}$.
5. Although the error bars for M42 and IC 4846 are almost consistent with the expected results for $[x(\text{O}^+)/x(\text{Fe}^+ + \text{Fe}^{++})]$ and $[x(\text{O}^{++})/x(\text{Fe}^{3+})]$, the results for the other objects and the fact that all the calculated results deviate in the same direction from the expected ones confirm that there is a significant deviation.
6. If the atomic data used in the models to derive the ionization balance of Fe were in error, the ionization fractions calculated for real objects could be used to obtain an estimate of the actual ICFs. The results in Figure 2 can be interpreted in such a way. A weighted least-squares fit to the data in Figure 2a leads to the following ICF,

$$\left[\frac{x(\text{O}^+)}{x(\text{Fe}^{++})} \right] = 0.78 \left(\frac{\text{O}^+}{\text{O}^{++}} \right)^{0.43}, \quad (4)$$

for $-1.5 \leq \log(\text{O}^+/\text{O}^{++}) \leq -0.5$, but the significance of the fit is not large, and other alternatives such as a constant $[x(\text{O}^+)/x(\text{Fe}^{++})] \simeq 0.25$, cannot be excluded.

In summary, there is a clear discrepancy between the calculated results and the model predictions. Even though the discrepancy might not be due to errors in the models (see §5 below), there are some problems with the models that would be worth exploring with further calculations. The ICFs selected here are in any case those leading to the lower discrepancies while at the same time being consistent with the model results.

5. DISCUSSION

There are three possible explanations for the discrepancy in the Fe abundances obtained from [Fe III] and [Fe IV]: (i) that the atomic data for [Fe IV] are unreliable; (ii) that the concentrations for the Fe ions predicted by photoionization models are greatly in error; and (iii) that there is some unknown mechanism producing a gradient in the Fe abundance within the ionized gas, as suggested by Bautista & Pradhan (1998). The high value of the discrepancy excludes other explanations, like errors in the line intensities, errors in the calculated physical conditions, or errors in the atomic data for [Fe III], which seem reliable, as discussed in §3.3. A contribution of fluorescence to [Fe III] emission can also be ruled out (Lucy 1995; Bautista & Pradhan 1998).

The [Fe IV] emissivities are almost insensitive to the values used for the transition probabilities and depend mainly on the values of the collision strengths. Therefore, to explain the discrepancies between the expected and calculated values for Fe^{3+} ($\text{Fe}_{\text{exp}}^{3+}/\text{Fe}^{3+}$ in Table 3), the simplest solution would be to lower all the collision strengths by a factor $\sim \text{Fe}_{\text{exp}}^{3+}/\text{Fe}^{3+}$. The values and errors given in Table 3 for the discrepancies imply that if the collision strengths were lower by a factor of ~ 5 , the Fe^{3+} abundances would be consistent with the expected values. On the other hand, there could be a difference between the discrepancies obtained for IC 4846 and M42 ($\text{Fe}_{\text{exp}}^{3+}/\text{Fe}^{3+} \sim 3.8$) and those for the other objects ($\text{Fe}_{\text{exp}}^{3+}/\text{Fe}^{3+} \sim 6$). This difference does not seem to arise from the fact that the T_e implied by the [O III] lines has been used to derive all the ionic abundances in SMC N88A and SBS 0335–052, whereas $T_e[\text{N II}]$ has been used in the other objects for deriving the abundances of the low ionization ions. An estimate of $T_e[\text{N II}]$ in SMC N88A and SBS 0335–052 can be obtained from $T_e[\text{O III}]$ and the relation derived by Campbell, Terlevich & Melnick (1986) from the models of Stasińska (1982). If these estimates of $T_e[\text{N II}]$ were used in the analysis, the discrepancies for SMC N88A and SBS 0335–052 would decrease, but by only a small amount to 5.1, 7.1 and 5.4 for SMC N88A bar, SMC N88A sq. A, and SBS 0335–052, respectively.

The Fe^{3+} abundance has been obtained for IC 4846 and M42 from the intensity of the line $[\text{Fe IV}] \lambda 6739.8$, whereas $[\text{Fe IV}] \lambda 2836.56$ and the $[\text{Fe IV}]$ blend at $\lambda 4904$ have been used for SMC N88A and SBS 0335–052 respectively. The upper level of the transition $[\text{Fe IV}] \lambda 6739.8$, $^2I_{11/2}$, is mainly populated by collisional excitations from the 4G levels, which are metastable. The levels $^4F_{7/2}$ and $^4F_{9/2}$, giving rise to the blend at $\lambda 4904$, are populated by collisional excitations from the 4G levels and from the ground state. The upper level of $[\text{Fe IV}] \lambda 2836.56$, $^4P_{5/2}$, is populated by spontaneous emission from the 4D term and by collisional excitations from both the 4G term and the ground state. The different discrepancies obtained from $[\text{Fe IV}] \lambda 6739.8$, on the one hand, and $[\text{Fe IV}] \lambda 2836.56$, $\lambda 4904$, on the other, could then be the effect of errors in the atomic data. As an example, if the collision strengths involving only the Fe^{3+} ground state were lowered by a factor of 6.5, the expected and calculated values of the Fe^{3+} abundance would differ by less than $\sim 50\%$. However, the difference in the discrepancies could be due to other causes. One possibility would be that the ICFs are highly dependent on metallicity; another, that the difference between the Fe abundances in the $[\text{Fe III}]$ and $[\text{Fe IV}]$ emitting regions depends on the metallicity or varies from object to object.

If the trend of increasing $[x(\text{O}^+)/x(\text{Fe}^{++})]$ with O^+/O^{++} suggested by the calculated data in Figure 2 were real, the Fe ionization fractions predicted by models should be seriously questioned. The value predicted by models for the relative concentrations of Fe^{++} and Fe^{3+} , $\text{Fe}^{++}/\text{Fe}^{3+}$, is roughly proportional to the ratio between the total recombination coefficient of Fe^{3+} and the ionization cross-section for Fe^{++} integrated over the radiation field. The latter ratio should then be higher by a factor ~ 5 to explain the discrepancy. The recent calculations of the ionization and recombination cross-sections for $\text{Fe}^{++}/\text{Fe}^{3+}$ (Nahar 1996a,b) are significantly different from the previous data. The new value for the total recombination coefficient for Fe^{3+} (Nahar 1996b) is a factor of 1.5 higher at $T_e \sim 10^4$ K than the previous value by Woods, Shull, & Sarazin (1981). On the other hand, the old values for the ionization cross-section of Fe^{++} (Reilman & Manson 1979) were calculated for energies above 35 eV and, when extrapolated to lower energies, lead to values which are higher than those calculated by Nahar (1996a) by a factor of 5 near the ionization threshold. However, according to Bautista & Pradhan (1998), this overestimation compensates in part for the contribution of the many resonant structures found by (Nahar 1996a) at low energies. Therefore, the new data finally lead to similar values for the ICFs—at least for the Orion model of Bautista & Pradhan (1998), as commented in §4 above. More extensive calculations exploring the effect of the new cross-sections for different degrees of ionization might be valuable. The effect of charge-exchange reactions, whose rates are highly uncertain (Kingdon & Ferland 1996), should also be explored. Such calculations will be the subject of future work.

An error in the calculations of the Fe ionization balance would prove to be the simplest

explanation for the trend in Figure 2. Some mechanism leading to the preferential destruction of dust grains in the low ionization zones could also explain such a trend, but this explanation seems rather ad hoc and less likely.

The accurate measurement of the relative intensities of several [Fe IV] lines in various objects where the physical conditions can also be measured with reasonable accuracy would help to distinguish between all these possibilities. These measurements could be attempted in low metallicity H II regions. The high T_e values prevailing in these objects boost the intensities of forbidden lines while the low metallicity reduces the possible contamination with permitted lines, an important issue when trying to measure very weak lines.

Figure 3 shows the values of the Fe/O abundance ratio obtained from the Fe^{++} abundance and an ICF (Figs. 3a and 3b) and from the Fe^{++} and Fe^{3+} abundances (Figs. 3c and 3d). The results are plotted as a function of the O abundance (Figs. 3a and 3c) and of the ionization degree O^+/O^{++} (Figs. 3b and 3d). The solar Fe/O and O/H abundance ratios are shown in Figure 3a as a dotted circle (Holweger 2001). The real value of the Fe/O abundance in the gas of a given object will be the result of two factors: the intrinsic value of Fe/O (in gas and dust) and the amount of Fe depleted in dust grains. The intrinsic value of Fe/O in a given object depends on the previous star formation history, but is expected to show less variation from object to object than either Fe/H or O/H. In stars of our Galaxy, Fe/O increases with metallicity and is 0.2 to 0.3 dex below solar when O/H is around 1 dex below solar (see, for example, Nissen et al. 2002). Abundance analyses of stars in the Magellanic clouds show the same increment but displaced by about 0.2 dex towards higher values of Fe/O at a given metallicity (Korn et al. 2000; Smith et al. 2002, and references therein). The intrinsic value of Fe/O in the interstellar medium of the Magellanic Clouds (that is, for SMC N88A and 30 Doradus) might then be solar or up to 0.2 dex above solar. The intrinsic value of Fe/O in SBS 0335–052 is not known. Chemical evolution models for another low metallicity dwarf galaxy, I Zw 18, predict values for Fe/O ranging from 0.1 dex above solar to about 0.7 dex below solar (see, for example, Recchi et al. 2002). This wide range of possible values arises from the uncertainties in both the star formation history and the iron yields due to massive stars, and makes it impossible to draw a conclusion on the most likely value for Fe/O in SBS 0335–052. On the other hand, good constraints on these two issues could be obtained from the real value of the Fe/O abundance ratio in SBS 0335–052 and other low metallicity blue compact galaxies. A low amount of dust within the ionized gas of these low metallicity objects can be inferred from the low or negligible extinction measured for them. Therefore, the higher value of Fe/O derived for SBS 0335–052 (the one obtained with [Fe III] emission and an ICF) favors a near solar value for the intrinsic Fe/O in the galaxy, whereas the lower Fe/O implied by [Fe IV] emission favors an intrinsic Fe/O about 0.7 dex below solar.

Figures 3b and 3d suggest an explanation for the different depletion factors of the objects in the sample. If IC 4846 (the only planetary nebula in the sample) is excluded, the values of Fe/O implied by both procedures increase with the degree of ionization. The same behavior was found in Rodríguez (1996, 2002) for Galactic H II regions with near solar metallicity and it was interpreted as due to the release of Fe atoms from dust grains by the action of energetic photons. The same process may be responsible for the low Fe depletion factors in SMC N88A and SBS 0335–052, but the amount of dust destruction and the slope of its dependence on the number of energetic photons depend strongly on which are the real values of Fe/O. Thus, the solution to the discrepancy found for [Fe IV] emission, has implications for both the chemical evolution of low metallicity galaxies and the evolution of dust in ionized nebulae.

6. CONCLUSIONS

The line [Fe IV] $\lambda 6739.8$ has been identified in published spectra of M42 and IC 4846. Upper limits to the intensity of this line and of [Fe IV] $\lambda 6734.4$ have been established for 30 Doradus. The tentative identification by Izotov et al. (2001) of a line at $\lambda \sim 4904$ in the spectra of SBS 0335–052 as an [Fe IV] feature has been confirmed. These data along with the measurement by Kurt et al. (1999) of [Fe IV] $\lambda 2836.56$ in two positions of SMC N88A have been used to perform an analysis of [Fe IV] emission in the five aforementioned nebulae. The Fe abundances obtained from [Fe III] lines and an ICF derived from ionization models, $\text{Fe}/\text{H} = 1.1 [(\text{Fe}^+ + \text{Fe}^{++})/\text{O}^+] \text{O}/\text{H}$, have been compared with those implied by the sum of the relevant ionic states, $\text{Fe}/\text{H} = \text{Fe}^+/\text{H}^+ + \text{Fe}^{++}/\text{H}^+ + \text{Fe}^{3+}/\text{H}^+$. The Fe/H abundance ratios obtained from the first method are higher than those derived from the second method by factors in the range 2.6–5.9. This result confirms the discrepancy previously found by Rubin et al. (1997) in M42 between the Fe abundance implied by [Fe II] and [Fe III] lines, and that implied by [Fe IV] $\lambda 2836.56$.

The Fe^{3+} abundance is systematically lower than expected for the five objects by factors from 3.2 to 7.5. The uncertainties in the derived discrepancy factors are too high to reach a definitive conclusion, but the present analysis offers two hints as to the possible explanation:

1. The discrepancies obtained with [Fe IV] $\lambda 6739.8$, on the one hand, and [Fe IV] $\lambda 2836.56$ and the [Fe IV] blend at $\lambda 4904$, on the other, might be different (see the values of $\text{Fe}_{\text{exp}}^{3+}/\text{Fe}^{3+}$ in Table 3). The measurement of these lines in a single object would help to establish this issue. If confirmed, this result would imply that the collision strengths for Fe^{3+} are unreliable.

2. The values of $[x(\text{O}^+)/x(\text{Fe}^{++})]$ derived for the objects in the sample might show a trend with the degree of ionization given by O^+/O^{++} (see Fig. 2). Since the ionization models predict a constant value for this ICF, $[x(\text{O}^+)/x(\text{Fe}^{++})] \simeq 1.1$, a deviation from this constant value that depends on the degree of ionization would suggest that the Fe ionization fractions predicted by models are seriously in error. The measurement of [Fe IV] lines in more objects would help to establish the reality of this trend.

Other explanations, like the existence of some kind of gradient in the Fe abundance within the ionized gas, cannot be ruled out at the moment.

The values of Fe/O implied by both methods decrease with metallicity, as shown in Figure 3. This trend, which should be confirmed for other low metallicity objects, probably reflects an increase of the Fe depletion factors in the different objects as their metallicity increases. The increment of Fe atoms in the gas of low metallicity H II regions could be due to the effect of the harder radiation fields typically found in these objects. This is suggested by the fact that if the planetary nebula IC 4846 is excluded, the Fe/O abundance ratios follow and extend to higher degrees of ionization the correlation with the degree of ionization previously found in Rodríguez (1996, 2002) for Galactic H II regions in the solar neighborhood. The deviation of IC 4846 from the relationship could be due to the large uncertainties in the abundances derived for this object or to the specific origin and characteristics of dust grains in planetary nebulae. Although the values of Fe/O for the other objects follow the correlation with the degree of ionization independently of whether [Fe IV] emission is considered or not, the shape of the correlation depends on which method is used in the abundance determination. Furthermore, the Fe/O abundance ratio in the low metallicity galaxy SBS 0335–052, which has important implications for our understanding of chemical evolution, remains uncertain by a factor of 5. All these implications emphasize the need for a correct understanding of the reasons behind the [Fe IV] discrepancy.

I thank R. Manso Sainz and R. H. Rubin for reading the paper and providing many useful comments, improvements and corrections. I also acknowledge discussions with L. Binette and the valuable comments of an anonymous referee. This work has made use of NASA's Astrophysics Data System Abstract Service. The project was supported by the Mexican CONACYT project J37680-E.

REFERENCES

- Baldwin, J. A., Ferland, G. J., Martin, P. G., Corbin, M. R., Cota, S. A., Peterson, B. M., & Slettebak, A. 1991, *ApJ*, 374, 580
- Baldwin, J. A., Verner, E. M., Verner, D. A., Ferland, G. J., Martin, P. G., Korista, K. T., & Rubin, R. H. 2000, *ApJS*, 129, 229
- Baluteau, J.-P., Zavagno, A., Morisset, C., & Péquignot, D. 1995, *A&A*, 303, 175
- Bautista, M. A., & Pradhan, A. K. 1998, *ApJ*, 492, 650
- Campbell, A., Terlevich, R., & Melnick, J. 1986, *MNRAS*, 223, 811
- Davey, A. R., Storey, P. J., & Kisielius, R. 2000, *A&AS*, 142, 85
- Esteban, C., Peimbert, M., Torres-Peimbert, S., & Rodríguez, M. 2002, *ApJ*, 581, 241
- Froese Fischer, C., & Rubin, R. H. 1998, *J. Phys. B: At. Mol. Opt. Phys.*, 31, 1657
- Garstang, R. H. 1958, *MNRAS*, 118, 572
- Gruenwald, R. B., & Viegas, S. M. 1992, *ApJS*, 78, 153
- Holweger, H. 2001, in *AIP Conf. Proc. 598, Solar and Galactic Composition*, ed. R. F. Wimmer-Schweingruber (New York: Springer-Verlag), 23
- Hyung, S., Aller, L. H., & Lee, W.-B. 2001, *PASP*, 113, 1559
- Izotov, Y. I., Chaffee, F. H., & Schaerer, D. 2001, *A&A*, 378, L45
- Izotov, Y. I., & Thuan, T. X. 1999, *ApJ*, 511, 639
- Kingdon, J. B., & Ferland, G. J. 1996, *ApJS*, 106, 205
- Korn, A. J., Becker, S. R., Gummersbach, C. A., & Wolf B. 2000, *A&A*, 353, 655
- Kurt, C. M., Dufour, R. J., Garnett, D. R., Skillman, E. D., Mathis, J. S., Peimbert, M., Torres-Peimbert, S., & Ruiz, M.-T. 1999, *ApJ*, 518, 246
- Lucy, L. B. 1995, *A&A*, 294, 555
- McKenna, F. C., Keenan, F. P., Hambly, N. C., Allende Prieto, C., Rolleston, W. R. J., Aller, L. H., & Feibelman, W. A. 1997, *ApJS*, 109, 225
- Nahar, S. 1996a, *Phys. Rev. A*, 53, 1545

- Nahar, S. 1996b, *Phys. Rev. A*, 53, 2417
- Nissen, P. E., Primas, F., Asplund, M., & Lambert, D. L. 2002, *A&A*, 390, 235
- Peimbert, A. 2003, *ApJ*, 584, 735
- Quinet, P. 1996, *A&AS*, 116, 573
- Recchi, S., Matteucci, F., D’Ercole, A., & Tosi, M. 2002, *A&A*, 384, 799
- Reilman, R. F., & Manson, S. T. 1979, *ApJS*, 40, 815
- Rodríguez, M. 1996, *A&A*, 313, L5
- Rodríguez, M. 1999a, *A&A*, 348, 222
- Rodríguez, M. 1999b, *A&A*, 351, 1075
- Rodríguez, M. 2002, *A&A*, 389, 556
- Rubin, R. H., Simpson, J. P., Haas, M. R., & Erickson, E. F. 1991a, *ApJ*, 374, 564
- Rubin, R. H., Simpson, J. P., Haas, M. R., & Erickson, E. F. 1991b, *PASP*, 103, 834
- Rubin, R. H., et al. 1997, *ApJ*, 474, L131
- Smith, V. V., et al. 2002, *AJ*, 124, 3241
- Stasińska, G. 1982, *A&AS*, 48, 299
- Stasińska, G. 1990, *A&AS*, 83, 501
- Verner, E. M., Verner, D. A., Baldwin, J. A., Ferland, G. J., & Martin, P. G. 2000, *ApJ*, 543, 831
- Woods, D. T., Shull, J. M., & Sarazin, C. L. 1981, *ApJ*, 249, 399
- Zhang, H. L. 1996, *A&AS*, 119, 523
- Zhang, H. L., & Pradhan, A. K. 1997, *A&AS*, 126, 373

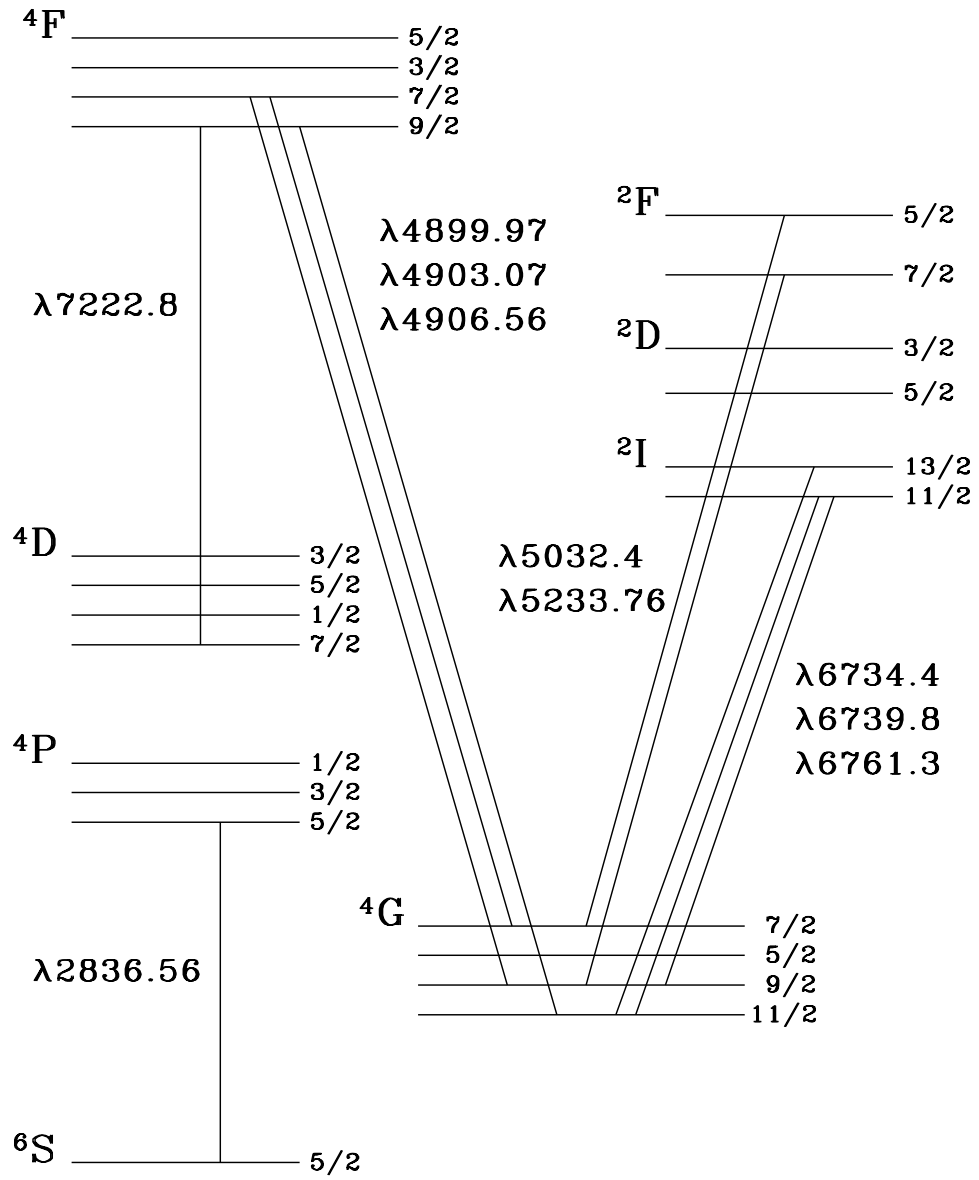


Fig. 1.— Schematic level diagram of Fe³⁺ up to 6.6 eV, with the transitions giving rise to the lines discussed in the text. Lines are labeled with air wavelengths except for the $\lambda 2836.56$ line, which is vacuum.

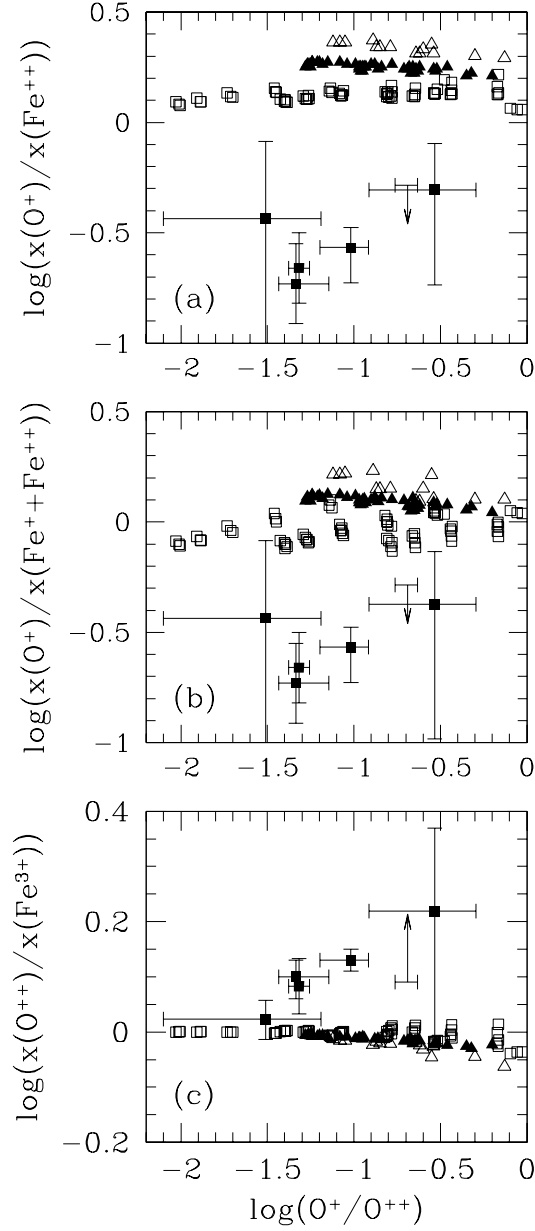


Fig. 2.— Values of different ratios between the ionization fractions of the Fe and O ions (the ICFs in eqs. [1], [2], and [3]) presented as a function of the degree of ionization given by O^+/O^{++} . The values calculated for IC 4846, M42, SMC N88A, and SBS 0335–052 are shown as filled squares; upper and lower limits are given for 30 Doradus, with the sizes of the arrows indicating a decrease by a factor of 2 in the Fe^{3+} abundance. The Fe^+ abundance has been considered negligible for all objects except M42. The empty squares are the results of the ionization models of Stasińska (1990). The triangles show the results of the models of Grunwald & Viegas (1992); empty triangles have been used for those models with solar metallicity, which deviate somewhat from the values for lower metallicities (the filled triangles). More information on the selected models is given in the text.

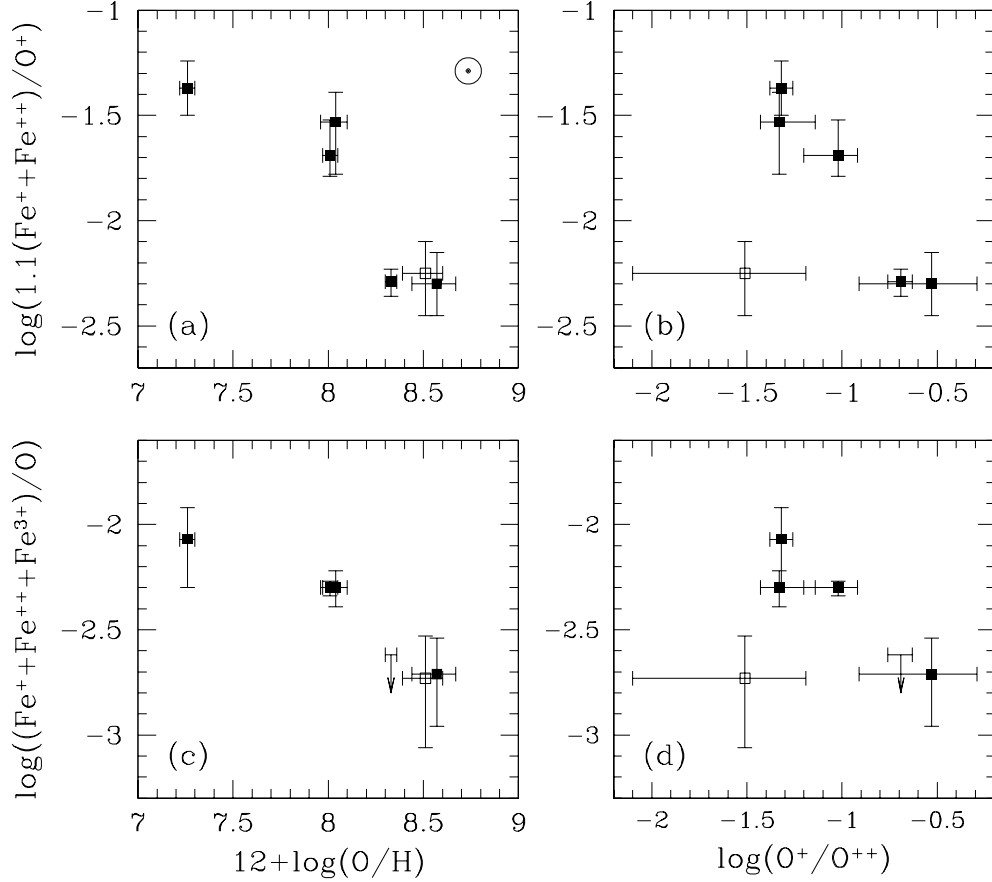


Fig. 3.— Fe/O abundance ratio as a function of the O abundance and the degree of ionization for M42, 30 Doradus, IC 4846, two positions in SMC N88A, and SBS 0335–052. The values for the planetary nebula IC 4846 are represented by an empty square. In panels (a) and (b) it has been assumed that $\text{Fe}/\text{O} = 1.1(\text{Fe}^+ + \text{Fe}^{++})/\text{O}^+$; panels (c) and (d) show the values obtained from $\text{Fe}/\text{O} = (\text{Fe}^+ + \text{Fe}^{++} + \text{Fe}^{3+})/\text{O}$. The contribution of Fe^+ has been considered negligible for all objects except M42. The dotted circle in panel (a) shows the solar abundances (Holweger 2001); the size of this symbol represents approximately the associated uncertainties.

Table 1. [Fe III] and [Fe IV] Lines and the Abundances of Fe⁺⁺ and Fe³⁺

[Fe III] Line	Fe ⁺⁺ /H ⁺					
	30 Doradus	IC 4846	M42	N88A bar	N88A sq. A	SBS 0335–052
$\lambda 4008$ (${}^3G_4 \rightarrow {}^5D_4$)	1.89E–7	...	3.08E–7
$\lambda 4080$ (${}^3G_4 \rightarrow {}^5D_3$)	3.44E–7
$\lambda 4607$ (${}^3F_3 \rightarrow {}^5D_4$)	1.64E–7
$\lambda 4658$ (${}^3F_4 \rightarrow {}^5D_4$)	1.59E–7	3.03E–8	3.13E–7	1.69E–7	1.31E–7	3.24E–8
$\lambda 4667$ (${}^3F_2 \rightarrow {}^5D_3$)	3.82E–7
$\lambda 4701$ (${}^3F_3 \rightarrow {}^5D_3$)	1.60E–7	...	3.15E–7
$\lambda 4734$ (${}^3F_2 \rightarrow {}^5D_2$)	1.75E–7	...	3.45E–7
$\lambda 4755$ (${}^3F_4 \rightarrow {}^5D_3$)	1.60E–7	...	3.21E–7	4.44E–8 ^a
$\lambda 4769$ (${}^3F_3 \rightarrow {}^5D_2$)	2.04E–7	...	3.17E–7
$\lambda 4778$ (${}^3F_2 \rightarrow {}^5D_1$)	1.41E–7	...	3.44E–7
$\lambda 4881$ (${}^3H_4 \rightarrow {}^5D_4$)	2.03E–7	3.79E–8	3.21E–7
$\lambda 4986$ (${}^3H_6 \rightarrow {}^5D_4$)	1.40E–7
$\lambda 5011$ (${}^3P_1 \rightarrow {}^5D_2$)	1.58E–7	...	3.10E–7
$\lambda 5084$ (${}^3P_1 \rightarrow {}^5D_0$)	3.44E–7
$\lambda 5270$ (${}^3P_2 \rightarrow {}^5D_3$)	1.69E–7	7.36E–8	3.07E–7
$\lambda 5412$ (${}^3P_2 \rightarrow {}^5D_1$)	1.48E–7	...	3.38E–7

[Fe IV] Line	Fe ³⁺ /H ⁺					
	30 Doradus	IC 4846	M42	N88A bar	N88A sq. A	SBS 0335–052
$\lambda 2837$ (${}^4P_{5/2} \rightarrow {}^6S_{5/2}$)	3.51E–7	4.17E–7	...
$\lambda 4900$ (${}^4F_{7/2} \rightarrow {}^4G_{9/2}$) ⁺						
$\lambda 4903$ (${}^4F_{7/2} \rightarrow {}^4G_{7/2}$) ⁺						
$\lambda 4907$ (${}^4F_{9/2} \rightarrow {}^4G_{11/2}$)	1.21E–7
$\lambda 5234$ (${}^2F_{7/2} \rightarrow {}^4G_{9/2}$)	1.39E–7 ^a
$\lambda 6734$ (${}^2I_{13/2} \rightarrow {}^4G_{11/2}$)	$\leq 4.70E-7$
$\lambda 6740$ (${}^2I_{11/2} \rightarrow {}^4G_{11/2}$)	$\leq 3.46E-7$	5.57E–7	3.36E–7
$\lambda 7223$ (${}^4F_{9/2} \rightarrow {}^4D_{7/2}$)	5.79E–8 ^a

Note. — The final adopted values and their uncertainties are listed in Table 2.

^aThese abundances have been derived from lines whose intensities are highly uncertain (Izotov et al. 2001) and are not used in the calculation of the final values.

Table 2. Physical Conditions and Ionic Abundances: $\{X\} = 12 + \log(X)$

Object	T_e^a (K)	N_e (cm^{-3})	$\{\text{O}^+/\text{H}^+\}$	$\{\text{O}^{++}/\text{H}^+\}$	$\{\text{Fe}^{++}/\text{H}^+\}$	$\{\text{Fe}^{3+}/\text{H}^+\}$
30 Doradus	10800^{+350}_{-300}	440 ± 190	$7.56^{+0.05}_{-0.06}$...	5.22 ± 0.07	...
	10000 ± 200	440 ± 190	...	8.25 ± 0.04	...	≤ 5.54
IC 4846	12200^{+5000}_{-2000}	8700 ± 3900	$6.99^{+0.31}_{-0.55}$...	$4.70^{+0.24}_{-0.60}$...
	10600^{+900}_{-600}	8700 ± 3900	...	$8.50^{+0.09}_{-0.12}$...	$5.75^{+0.20}_{-0.34}$
M42	10000^{+1600}_{-1000}	6400 ± 2800	$7.92^{+0.23}_{-0.32}$...	$5.52^{+0.16}_{-0.20}$...
	8300^{+600}_{-400}	6400 ± 2800	...	$8.46^{+0.11}_{-0.15}$...	$5.52^{+0.24}_{-0.46}$
N88A bar	14200 ± 400	10200^{+4800}_{-6100}	$6.96^{+0.11}_{-0.19}$	7.97 ± 0.04	5.23 ± 0.05	5.55 ± 0.06
N88A sq. A	13500^{+900}_{-600}	1500^{+4500}_{-1000}	$6.69^{+0.19}_{-0.14}$	$8.02^{+0.06}_{-0.08}$	$5.12^{+0.11}_{-0.13}$	$5.62^{+0.11}_{-0.16}$
SBS 0335–052	20200^{+800}_{-700}	300^{+400}_{-270}	$5.92^{+0.06}_{-0.07}$	$7.24^{+0.03}_{-0.04}$	4.51 ± 0.11	$5.08^{+0.18}_{-0.32}$

^aWhen two values are given for T_e , the first one is that derived from the [N II] lines; the second value is from the [O III] lines. A single entry shows the T_e obtained from the [O III] lines.

Table 3. Total Abundances: $\{X\} = 12 + \log(X)$

Object	{O/H}	{Fe/H} ^a	log Fe/O ^a	{Fe/H} ^b	log Fe/O ^b	Fe _{exp} ³⁺ /Fe ³⁺ ^c
30 Doradus	8.33±0.03	6.04±0.07	-2.29 ^{+0.06} _{-0.07}	≤ 5.71	≤ -2.62	≥ 2.7
IC 4846	8.51 ^{+0.09} _{-0.12}	6.26 ^{+0.16} _{-0.25}	-2.25 ^{+0.15} _{-0.20}	5.78 ^{+0.19} _{-0.30}	-2.73 ^{+0.20} _{-0.33}	3.2 ^{+2.3} _{-2.4}
M42	8.57 ^{+0.10} _{-0.13}	6.27 ^{+0.19} _{-0.22}	-2.30±0.15	5.86 ^{+0.15} _{-0.20}	-2.71 ^{+0.17} _{-0.25}	4.4 ^{+4.1} _{-3.9}
N88A bar	8.01±0.04	6.32 ^{+0.15} _{-0.10}	-1.69 ^{+0.17} _{-0.10}	5.72±0.05	-2.30 ^{+0.03} _{-0.04}	5.5 ^{+2.5} _{-1.3}
N88A sq. A	8.04 ^{+0.06} _{-0.08}	6.51 ^{+0.14} _{-0.24}	-1.53 ^{+0.14} _{-0.25}	5.74 ^{+0.10} _{-0.13}	-2.30 ^{+0.08} _{-0.09}	7.5 ^{+3.2} _{-3.6}
SBS 0335–052	7.26±0.04	5.89 ^{+0.13} _{-0.14}	-1.37±0.13	5.19 ^{+0.15} _{-0.23}	-2.07 ^{+0.15} _{-0.23}	6.1 ^{+3.7} _{-3.5}

^aFe/H = 1.1 [(Fe⁺ + Fe⁺⁺)/O⁺] O/H.

^bFe/H = Fe⁺/H⁺ + Fe⁺⁺/H⁺ + Fe³⁺/H⁺.

^cThe ratio between the expected and calculated values of Fe³⁺/H⁺, where Fe_{exp}³⁺/H⁺ is derived from Fe⁺/H⁺ + Fe⁺⁺/H⁺ + Fe_{exp}³⁺/H⁺ = 1.1 [(Fe⁺ + Fe⁺⁺)/O⁺] O/H.